Inorganic Chemistry

including bioinorganic chemistry

December 1, 2014
Volume 53, Number 23
pubs.acs.org/IC

Intermediate Spin in Organocobalt(III) Chemistry

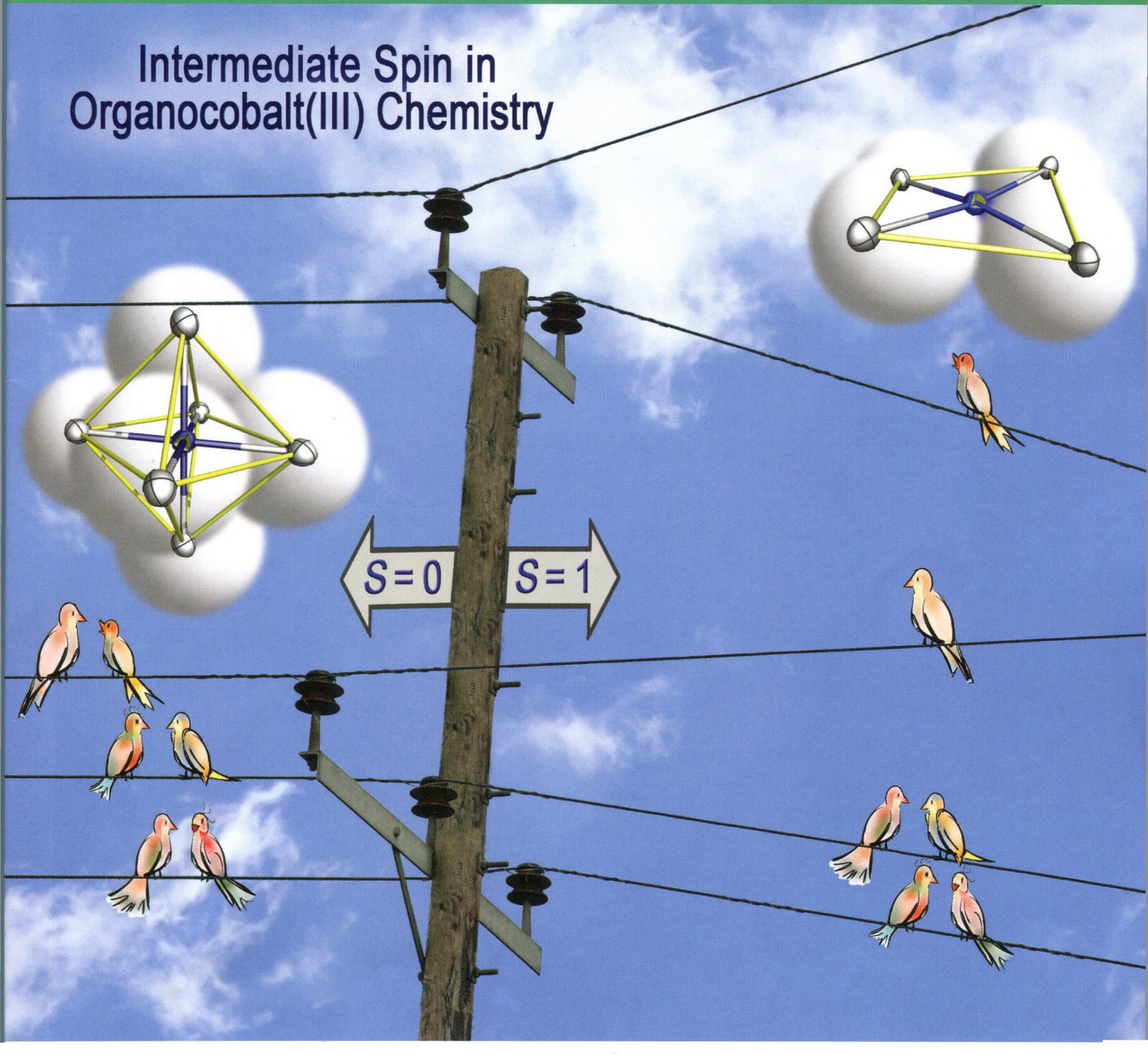

ACS Publications
Most Trusted. Most Cited. Most Read.

www.acs.org

Inorganic Chemistry

DECEMBER 1, 2014
VOLUME 53 ISSUE 23

INOCAJ 53(23) 12225–12664 (2014)
ISSN 0020-1669

ON THE COVER: Octahedral cobalt(III) compounds are almost exclusively diamagnetic ($S = 0$). In a square-planar environment, however, sizable d_z^2-orbital stabilization occurs, enabling an intermediate spin state ($S = 1$). Such an open-shell electron configuration, which is unprecedented in organocobalt(III) chemistry, has now been substantiated in homoleptic $[NBu_4][CoR_4]$ compounds (R = C_6F_5, C_6Cl_5). See M. A. García-Monforte, I. Ara, A. Martín, B. Menjón, M. Tomás, P. J. Alonso, A. B. Arauzo, J. I. Martínez, and C. Rillo, p 12384.

Communications

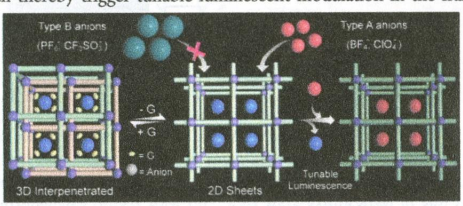

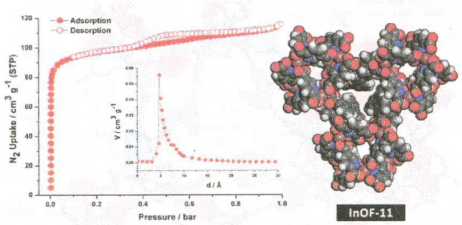

12231 S

DOI: 10.1021/ic501965m

Structure and Properties of Neutral and Cationic Gold(III) Complexes from Substituted 2-(2′-Pyridyl)quinoline Ligands

Edward M. Laguna, Pauline M. Olsen, Michael D. Sterling, Jack F. Eichler, Arnold L. Rheingold, and Catharine H. Larsen*

A one-step, green catalytic synthesis of substituted 2-(2′-pyridyl)quinolines provides ligands bearing electron-donating to electron-withdrawing groups. Neutral and cationic gold(III) complexes of these bidentate heteroaromatic ligands were studied and characterized by single-crystal X-ray diffraction, NMR, IR, high-resolution mass spectrometry, and elemental analysis. Whereas the four-coordinate cationic gold(III) chloride complex has a distorted square-planar ligand environment, neutral gold(III) chloride complexes from substituted 2-(2′-pyridyl)quinoline ligands display an additional axial interaction.

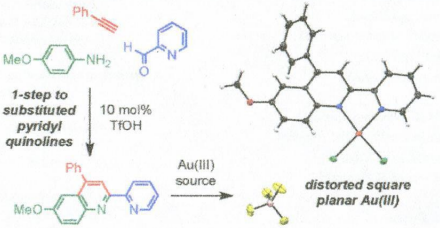

12234 S

DOI: 10.1021/ic502042h

Three-Dimensional Frameworks Based on Dodecanuclear Dy–hydroxo Wheel Cluster with Slow Relaxation of Magnetization

Yi-Xia Ren, Xiang-Jun Zheng,* Li-Cun Li,* Da-Qiang Yuan, Miao An, and Lin-Pei Jin

Two new coordination polymers possessing a wheel-cluster core based on four vertex-sharing cubane-like $[Ln_4(\mu_3\text{-}OH)_4]^{8+}$ units were prepared. The Dy_{12} cores are linked by 2-sulfoterephthalate ligands into a three-dimensional (3D) architecture with slow relaxation of magnetization, and it can be regarded as the first 3D coordination assembly of Dy_{12} cluster single-molecule magnet.

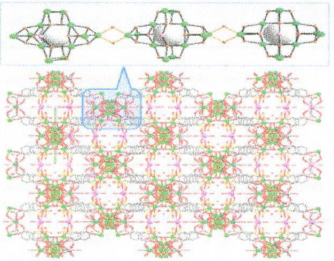

12237 S

DOI: 10.1021/ic502267t

Reductive Silylation of the Uranyl Ion with Ph_3SiOTf

Elizabeth A. Pedrick, Guang Wu, and Trevor W. Hayton*

The reaction of Ph_3SiOTf with $UO_2(dbm)_2(THF)$ (dbm = $OC(Ph)CHC(Ph)O$) and $UO_2(^{Ar}acnac)_2$ ($^{Ar}acnac$ = $ArNC(Ph)CHC(Ph)O$; Ar = 3,5-$^tBu_2C_6H_3$) results in the one-electron reduction of the U center, concomitant with silylation of both oxo ligands.

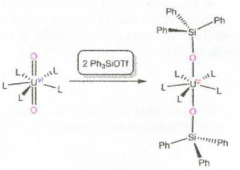

12240 S DOI: 10.1021/ic502564r

Synthesis and Spectroscopic Characterization of High-Spin Mononuclear Iron(II) *p*-Semiquinonate Complexes

Amanda E. Baum, Heaweon Park, Sergey V. Lindeman, and Adam T. Fiedler*

Mononuclear iron(II) complexes featuring *p*-semiquinonate ligands are generated via the reduction of coordinated quinones and characterized with spectroscopic methods.

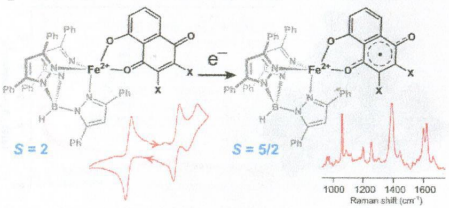

Articles

12243 S DOI: 10.1021/ic500354t

Structural, Spectroscopic, and Magnetic Properties of Eu^{3+}-Doped $GdVO_4$ Nanocrystals Synthesized by a Hydrothermal Method

Agata Szczeszak, Tomasz Grzyb, Zbigniew Śniadecki, Nina Andrzejewska, Stefan Lis,* Michał Matczak, Grzegorz Nowaczyk, Stefan Jurga, and Bogdan Idzikowski

Nanocrystalline gadolinium orthovanadates doped with Eu^{3+} ions were synthesized in situ by a hydrothermal method. Structural and detailed spectroscopic analyses based on luminescence spectra and decay curves of the synthesized nanophosphors were done. The magnetic properties of the bifunctional nanophosphors were studied by measurements of the dependence of the magnetization on magnetic field and temperature.

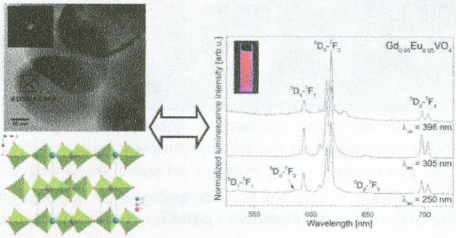

12253 S DOI: 10.1021/ic500791m

Ab Initio Investigation of the UO_3 Polymorphs: Structural Properties and Thermodynamic Stability

Nicholas A. Brincat, Stephen C. Parker,* Marco Molinari, Geoffrey C. Allen, and Mark T. Storr

We present a comprehensive PBE + U treatment of the UO_3 polymorphs, assessing structural, electronic, and elastic properties as well as relative stability. Good agreement with experiment is found, and the properties are linked to the presence or absence of a uranyl bond.

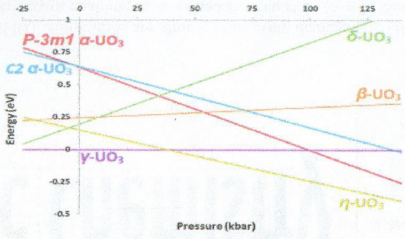

12265 S DOI: 10.1021/ic5011693

Field-Induced Spin-Flop in Antiferromagnetic Semiconductors with Commensurate and Incommensurate Magnetic Structures: Li_2FeGeS_4 (LIGS) and Li_2FeSnS_4 (LITS)

Jacilynn A. Brant, Clarina dela Cruz, Jinlei Yao, Alexios P. Douvalis, Thomas Bakas, Monica Sorescu, and Jennifer A. Aitken*

Divalent ions are directed to specific locations within the structures of the Li_2–Fe–IV–S_4 diamond-like materials to generate antiferromagnetic ordering. Both compounds undergo a reversible spin-flop transition. Changing the tetravalent ion in these materials alters the bandgaps and magnetic structures. The indirect-gap (E_g = 1.4 eV) semiconductor Li_2FeGeS_4 has a magnetic structure that is commensurate with the nuclear structure, while Li_2FeSnS_4 has a direct bandgap (E_g = 1.9 eV) and an incommensurate magnetic structure.

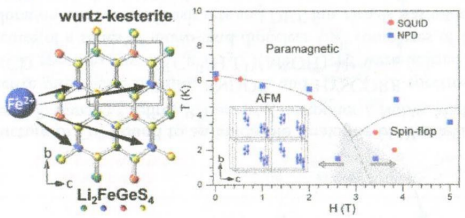

12275 S DOI: 10.1021/ic501252x

Eu(III) and Tb(III) Complexes with the Nonsteroidal Anti-Inflammatory Drug Carprofen: Synthesis, Crystal Structure, and Photophysical Properties

Xianju Zhou,* Xiaoqi Zhao, Yongjie Wang, Bing Wu, Jun Shen, Li Li, and Qingxu Li

Tb complex with the nonsteroidal anti-inflammatory drug carprofen presents intense green emission through the antenna effect of the ligand.

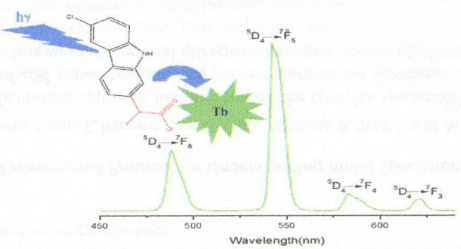

12283 S DOI: 10.1021/ic501400n

From Chromium–Chromium Quintuple Bonds to Molecular Squares and Porous Coordination Polymers

Awal Noor, Emmanuel Sobgwi Tamne, Benjamin Oelkers, Tobias Bauer, Serhiy Demeshko, Franc Meyer, Frank W. Heinemann, and Rhett Kempe*

Reaction of a quintuply bonded chromium(I) dimer with 4,4′-bipyridine completely cleaves the metal–metal bond, leading to a chromium(II)-based molecular square. Controlled polymerization of this compound with pyrazine yields a porous coordination polymer (PCP) featuring both reduced and nonreduced linkers.

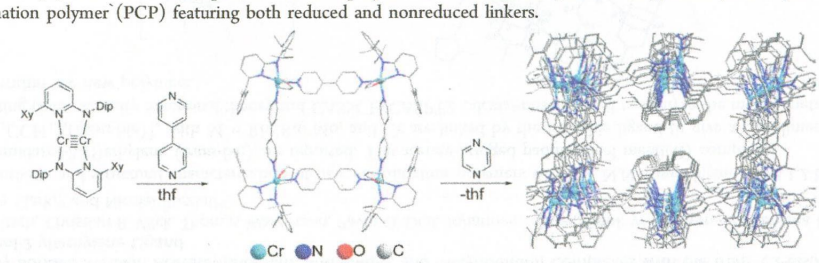

12289 S

DOI: 10.1021/ic5014126

One Pot, Two Phases: Individual Orthorhombic and Face-Centered Cubic $ZnSnO_3$ Obtained Synchronously in One Solution

Ying Wang, Peng Gao,* Di Bao, Longqiang Wang, Yujin Chen,* Xiaoming Zhou, Piaoping Yang,* Shuchao Sun, and Milin Zhang

The topic of obtaining pure crystals from the concomitant allotropes is ever before the eyes of numerous researchers. As a typical example, well-defined individual face-centered cubic and orthorhombic $ZnSnO_3$ microspheres were successfully synthesized, assisted by a ZnO inducing template or without it in an identical solution, respectively.

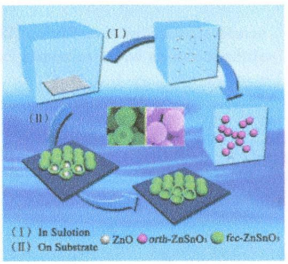

12297

DOI: 10.1021/ic501371d

Structural Properties and Singular Phase Transitions of Metallic $Pr_{0.50}Sr_{0.50}CoO_3$ Cobaltite

Jessica Padilla-Pantoja, José Luis García-Muñoz,* Bernat Bozzo, Zdeněk Jirák, and Javier Herrero-Martín

The $Pr_{0.50}Sr_{0.50}CoO_3$ perovskite exhibits unique magnetostructural properties among the rest of the ferromagnetic/metallic $Ln_{0.50}Sr_{0.50}CoO_3$ compounds. We have determined and described its structural evolution, which follows the $Pm\bar{3}m \rightarrow R\bar{3}c \rightarrow Imma \rightarrow I4/mcm$ transformations. The $Imma \rightarrow I4/mcm$ symmetry change is responsible for the second magnetic transition and the reported "two-step magnetic ordering" and has been thoroughly described. The results are confronted with distinct nonconventional properties in another half-doped cobaltite based on praseodymium, $Pr_{0.50}Ca_{0.50}CoO_3$.

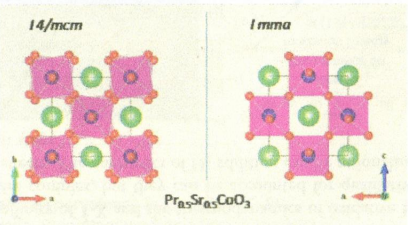

12305 S DOI: 10.1021/ic501435a

Multiply Bonded Metal(II) Acetate (Rhodium, Ruthenium, and Molybdenum) Complexes with the *trans*-1,2-Bis(*N*-methylimidazol-2-yl)ethylene Ligand

Nico Fritsch, Christian R. Wick, Thomas Waidmann, Pavlo O. Dral, Johannes Tucher, Frank W. Heinemann, Tatyana E. Shubina, Timothy Clark,* and Nicolai Burzlaff*

The synthesis and structural characterization of new coordination polymers with the N,N-donor ligand *trans*-1,2-bis(*N*-methylimidazol-2-yl)ethylene (*trans*-bie) are reported. The acetate-bridged paddlewheel metal(II) complexes $[M_2(O_2CCH_3)_4(trans\text{-bie})]_n$ with M = Rh, Ru, Mo, and Cr are linked by the *trans*-bie ligand to give a one-dimensional alternating chain. Density functional theory and CASSCF/CASPT2 calculations are used to analyze the metal−metal multiple bonds within the new polymers.

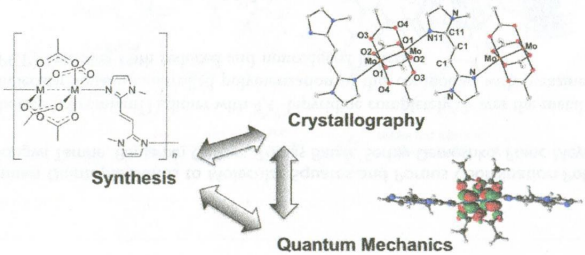

12315 S DOI: 10.1021/ic501408r

Integrated Computational and Experimental Protocol for Understanding Rh(III) Speciation in Hydrochloric and Nitric Acid Solutions

Alex C. Samuels, Cherilynn A. Boele, Kevin T. Bennett, Sue B. Clark, Nathalie A. Wall,* and Aurora E. Clark*

A combined experimental and theoretical approach has investigated the complex speciation of Rh(III) in hydrochloric and nitric acid media, as a function of acid concentration. This has relevance to the separation and isolation of Rh(III) from dissolved spent nuclear fuel, which is an emergent and attractive alternative source of platinum group metals, relative to traditional mining efforts.

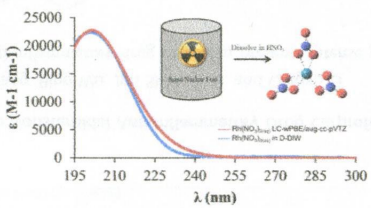

12323 S DOI: 10.1021/ic5014413

Insights into the Electronic Structure of Cu^{II} Bound to an Imidazole Analogue of Westiellamide

Peter Comba, Nina Dovalil, Graeme R. Hanson,* Jeffrey R. Harmer, Christopher J. Noble, Mark J. Riley, and Bjoern Seibold

High-resolution orientation-selective three-pulse ESEEM, ENDOR, and HYSCORE spectroscopy in conjunction with computational chemistry and MCD spectroscopy of $[Cu^{II}(H_2L^1)(MeOH)_2)]^+$ were utilized to determine the molecular (geometric and electronic) structure of a series of mono- and dinuclear Cu^{II} complexes of three synthetic analogues of Westiellamide. A systematic exploration of a range of basis sets and DFT functionals was undertaken to determine their ability to reproduce the experimentally determined spin Hamiltonian parameters.

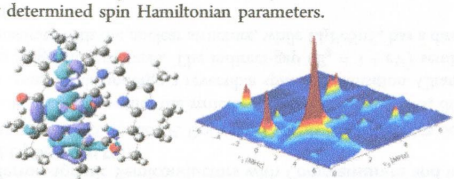

12337 S

DOI: 10.1021/ic5014973

pH and Ligand Dependent Assembly of Well–Dawson Arsenomolybdate Capped Architectures

He Zhang, Kai Yu,* Chunmei Wang, Zhanhua Su, Chunxiao Wang, Di Sun, Honghong Cai, Zhaoyi Chen, and Baibin Zhou*

Certain numbers of Cu^{2+} and As^{3+} are introduced into a Dawson $\{As_2Mo_{18}\}$ system to act as cap by self-assembly reaction of $NaAsO_2$ as raw material, which lead to five novel arsenomolybdates. The electrocatalytic, magnetic, and fluorescent properties of title compounds have been investigated in detail.

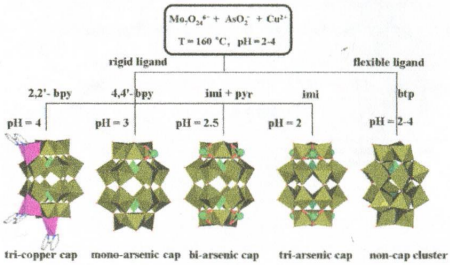

12348 S

DOI: 10.1021/ic5015829

Calculation of Ionization Energy, Electron Affinity, and Hydride Affinity Trends in Pincer-Ligated d^8-Ir(^{tBu4}PXCXP) Complexes: Implications for the Thermodynamics of Oxidative H_2 Addition

Abdulkader Baroudi, Ahmad El-Hellani, Ashfaq A. Bengali, Alan S. Goldman, and Faraj Hasanayn*

The ionization energy and electron affinity of **1**-X and the thermodynamics of oxidative H_2 addition are obtained from DFT calculations. The computed trends are complex, but they can be accounted for qualitatively by invoking a combination of electronegativity and specific π-MO effects. The energetics of H_2 addition can be rationalized on the basis of consideration of a cycle of hydride and proton addition steps.

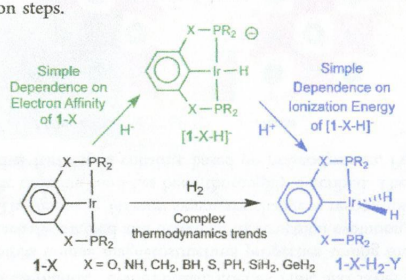

12360 DOI: 10.1021/ic501600s

Ag(I) and Tl(I) Precursors as Transfer Agents of a Pyrrole-Based Pincer Ligand to Late Transition Metals

Julie A. Kessler and Vlad M. Iluc*

Thallium and silver species of a pyrrole-based PNP pincer were paramount in the formation of new iridium and ruthenium complexes, which could not be isolated using the protonated pro-ligand or the corresponding lithium pyrrolide salt. Interestingly, the thallium complex is low-coordinated in the solid state, showing no binding to the phosphine donors and weak η^2 intermolecular interactions to the backbone of a neighboring pyrrole molecule, a structure supported by DFT calculations.

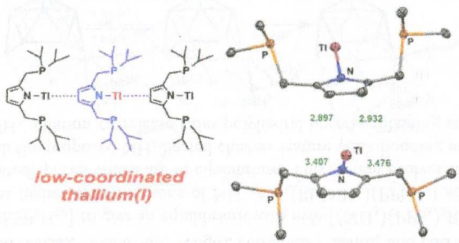

12372 DOI: 10.1021/ic501695n

Kinetic Effects of Sulfur Oxidation on Catalytic Nitrile Hydration: Nitrile Hydratase Insights from Bioinspired Ruthenium(II) Complexes

Davinder Kumar, Tho N. Nguyen, and Craig A. Grapperhaus*

Nitrile hydratase inspired kinetic investigations on a series of Ru nitrile hydration catalysts reveal that sulfur oxidation promotes nitrile binding and its polarization and proceeds through a highly ordered transition state. Thermodynamic studies reveal that sulfur oxidation significantly lowers the enthalpic barrier of the reaction, and the experimental findings are well-reproduced by DFT studies.

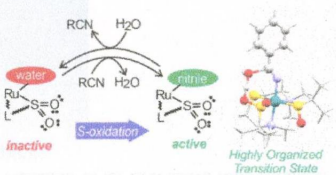

12378 DOI: 10.1021/ic501708b

Thermochromism in Yttrium Iron Garnet Compounds

Hélène Serier-Brault,* Lucile Thibault, Magalie Legrain, Philippe Deniard, Xavier Rocquefelte, Philippe Leone, Jean-Luc Perillon, Stéphanie Le Bris, Jean Waku, and Stéphane Jobic*

This work evidences a thermochromic behavior of yttrium iron garnet, from greenish to brownish, by applying a temperature variation. This color change originates from a continuous red shift of the O^{2-}—Fe^{3+} ligand-to-metal charge transfer, whereas no impact on the d—d transition is observed. Doping with Cr^{3+} cations was also investigated to obtain more saturated colors.

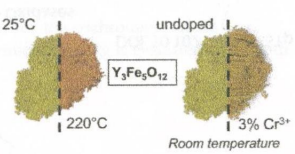

12384 S

DOI: 10.1021/ic501719y

Homoleptic Organocobalt(III) Compounds with Intermediate Spin

M. Angeles García-Monforte, Irene Ara, Antonio Martín, Babil Menjón,* Milagros Tomás, Pablo J. Alonso,* Ana B. Arauzo, Jesús I. Martínez, and Conrado Rillo

The homoleptic species $[NBu_4][Co^{III}R_4]$ (R = C_6F_5, C_6Cl_5) are the first organocobalt(III) compounds with square-planar structure. According to this tetragonal geometry with no axial interactions, their magnetic properties reveal an intermediate-spin (spin triplet) ground state.

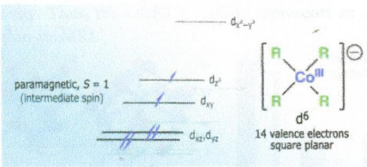

12396 S

DOI: 10.1021/ic501664x

Hydrothermal Preparation and Magnetic Properties of $NaFeSi_2O_6$: Nanowires vs Bulk Samples

Shiliang Zhou, Wolfgang G. Zeier, Moureen C. Kemei, Moulay T. Sougrati, Matthew Mecklenburg, and Brent C. Melot*

A low-temperature hydrothermal route is reported to prepare $NaFeSi_2O_6$ nanowires with high purity. A comparative study on the $NaFeSi_2O_6$ nanowires and the bulk samples reveals distinct differences in their magnetic properties.

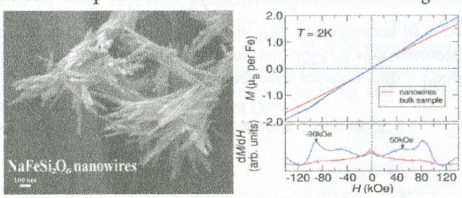

12402

DOI: 10.1021/ic502436a

Nature of Holes, Oxidation States, and Hypervalency in Covellite (CuS)

Sergio Conejeros, Ibério de P. R. Moreira, Pere Alemany,* and Enric Canadell*

Analysis of the electronic structure reveals the important role of S−S bonds and hypervalent sulfur in understanding the bonding and oxidation formalism for metallic covellite (CuS).

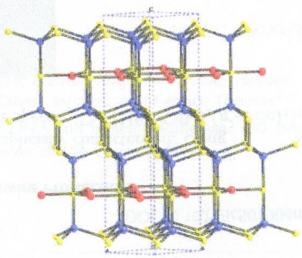

12407 S DOI: 10.1021/ic5017559

Ru–Zn Heteropolynuclear Complexes Containing a Dinucleating Bridging Ligand: Synthesis, Structure, and Isomerism

Lorenzo Mognon, Jordi Benet-Buchholz, S. M. Wahidur Rahaman, Carles Bo,* and Antoni Llobet*

The coordination chemistry of new dinuclear Ru–Zn and self-assembled heterotrinuclear Ru_2–Zn complexes that contain the Hbpp ligand have been thoroughly characterized by means of spectroscopic and electrochemical techniques. Additionally, a light-induced linkage isomerization reaction has been shown to occur for the Ru–Cl heterotrinculear complexes.

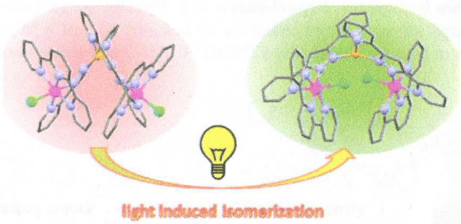

12416 S DOI: 10.1021/ic501751p

Molybdenum Complex with Bulky Chelates as a Functional Model for Molybdenum Oxidases

Jana Leppin, Christoph Förster, and Katja Heinze*

The dioxidomolybdenum complex $Mo^{VI}(^{iPr2}\mathbf{L})_2O_2$ with the bulky chelate ligand [(4,5-diisopropyl-1*H*-pyrrole-2-yl)-methylene]-4-(*tert*-butyl)aniline is active in oxygen-atom transfer to PR_3, yielding OPR_3 (R = Me, Ph). No dinuclear complex $[Mo^{V}(^{iPr2}\mathbf{L})_2O]_2(\mu\text{-}O)$ is observed. Instead, PMe_3 strongly coordinates to Mo^{IV}, while PPh_3 and $OPPh_3$ are only weakly associated. The latter species readily reacts with water and dioxygen under chelate dissociation to give diamagnetic $[Mo^{V}(^{iPr2}\mathbf{L})O]_2(\mu\text{-}O)_2$. From the PMe_3 complex, the phosphane is liberated by oxidation to an EPR-active Mo^{V} complex.

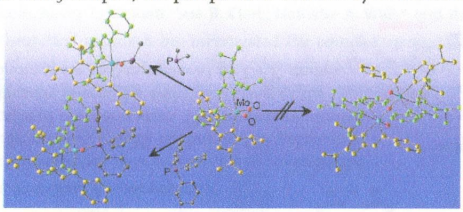

12428 S DOI: 10.1021/ic501779n

NH_3-Promoted Ligand Lability in Eleven-Vertex Rhodathiaboranes

Beatriz Calvo, Beatriz Roy, Ramón Macías,* Maria Jose Artigas, Fernando J. Lahoz, and Luis A. Oro

NH_3 reacts with *nido*-$[(PPh_3)_2RhSB_9H_{10}]$ to give an equilibrium with *nido*-$[(NH_3)(PPh_3)_2RhSB_9H_{10}]$ that involves ammonia coordination and dissociation. At higher concentrations of NH_3, the $\{Rh(NH_3)(PPh_3)_2\}$ adduct undergoes PPh_3 ligand dissociation giving new NH_3-ligated species which are in equilibrium. This system evolves to form a hydridorhodathiaborane that features a H_3N–B group. All the proposed NH_3-ligated clusters feature weak-bonding interactions with ammonia closing a rare stoichiometric cycle of NH_3 addition to/release from polyhedral boron-containing compounds.

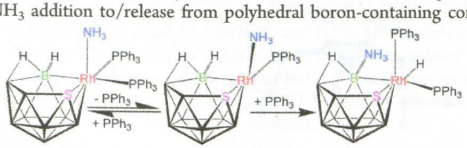

12437 S

DOI: 10.1021/ic5018054

Pyrazolylamidino Ligands from Coupling of Acetonitrile and Pyrazoles: A Systematic Study

Patricia Gómez-Iglesias, Marta Arroyo, Sonia Bajo, Carsten Strohmann, Daniel Miguel, and Fernando Villafañe*

Mixed pyrazole–acetonitrile complexes, both neutral *fac*-[ReBr(CO)$_3$(NCMe)(pz*H)] (pz*H = pzH, pyrazole; dmpzH, 3,5-dimethylpyrazole; or indzH, indazole) and cationic *fac*-[Re(CO)$_3$(NCMe)(pz*H)$_2$]A (A = BF_4, ClO_4, or OTf), are described. Their role as the only starting products to obtain final pyrazolylamidino complexes *fac*-[ReBr(CO)$_3$(NH=C(Me)pz*-κ^2*N,N*)] and *fac*-[Re(CO)$_3$(pz*H)(NH=C(Me)pz*-κ^2*N,N*)]A, respectively, is examined. Other products involved in the processes, such as *fac*-[ReBr(CO)$_3$(pz*H)$_2$], *fac*-[Re(CO)$_3$(NCMe)(NH=C(Me)pz*-κ^2*N,N*)]A, and *fac*-[Re(CO)$_3$(pz*H)$_2$(OTf)], are also described.

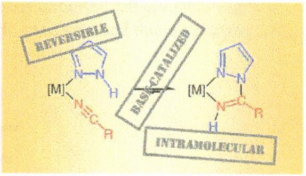

12449 S

DOI: 10.1021/ic501904m

Synthesis and Structural Characterization of Group 4 Metal Carboxylates for Nanowire Production

Timothy J. Boyle,* Daniel T. Yonemoto, Thu Q. Doan, and Todd M. Alam

A series of carboxylic acid group 4 precursors have been synthesized and crystallographcially characterized. Using electrospinning, ceramic nanowires without polymer additions were observed for some species. The [Hf(μ-OBc)$_2$(η^2-OBc)$_2$]$_2$ derivative (shown) yields a porous wire (TEM shown) upon ES processing.

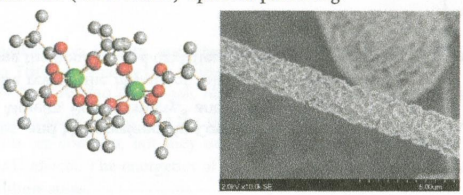

12459 S

DOI: 10.1021/ic5018714

Lead(II) Binding to the Chelating Agent D-Penicillamine in Aqueous Solution

Natalie S. Sisombath, Farideh Jalilehvand,* Adam C. Schell, and Qiao Wu

Lead(II) ion forms a Pb(penicillamine)$_2$ complex in alkaline aqueous solution with a PbS_2NO coordination environment, characterized for the first time by ^{207}Pb- and ^{13}C NMR, UV-vis, and EXAFS spectroscopic techniques. Formation of such Pb(*S,N,O*-Pen)(*S*-Cys) complexes *in vivo* could be important in lead detoxification by D-penicillamine.

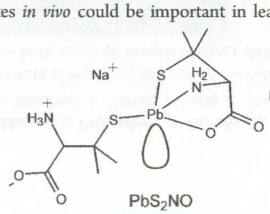

Pb-S ave. = 2.64 ± 0.04 Å

Pb-(N/O) ave. = 2.45 ± 0.04 Å

δ (^{207}Pb) ~1870 ppm

λ_{max} = 298 nm

12469 S DOI: 10.1021/ic501895s

Ruthenium Hydrides Containing the Superhindered Polydentate Polyphosphine Ligand $P(CH_2CH_2P^tBu_2)_3$

Ryan Gilbert-Wilson, Leslie D. Field,* and Mohan Bhadbhade

The complex $RuH_2(N_2)(P^2P_3^{tBu})$ (**1**) containing the extremely bulky PP_3-type ligand $P^2P_3^{tBu} = P(CH_2CH_2P^tBu_2)_3$ was synthesized by reduction of $RuCl_2(P^2P_3^{tBu})$ (**2**) with Na/NH_3 under a N_2 atmosphere. Like other complexes containing the $P^2P_3^{tBu}$ ligand, only three of the four donor phosphines are coordinated, and one of the phosphines remains as a dangling pendant ligand. Reduction of $RuCl_2(P^2P_3^{tBu})$ (**2**) with the usual hydride reducing agents afforded the previously unknown ruthenium hydride complexes $RuHCl(P^2P_3^{tBu})$, $RuH(BH_4)(P^2P_3^{tBu})$, $RuH(AlH_4)(P^2P_3^{tBu})$, and the ruthenium(II) trihydride $K[Ru(H)_3(P^2P_3^{tBu})]$.

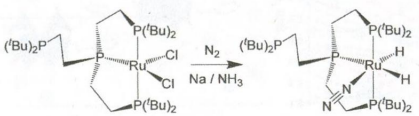

2 1

12480 S DOI: 10.1021/ic5019168

Solid State Isostructural Behavior and Quantified Limiting Substitution Kinetics in Schiff-Base Bidentate Ligand Complexes *fac*-[Re(*O,N*-Bid)(CO)$_3$(MeOH)]^n

Alice Brink, Hendrik G. Visser, and Andreas Roodt*

A range of *fac*-$[Re(CO)_3(O,N\text{-Bid})(H_2O)]^n$ (*O,N*-Bid = monoanionic Schiff bases with different imine nitrogen functionalities), and the methanol substitution by a range of monodentate entering pyridine type nucleophiles (L), are reported, yielding a systematic quantified dependence of the dissociative interchange equilibrium and rate constants on L.

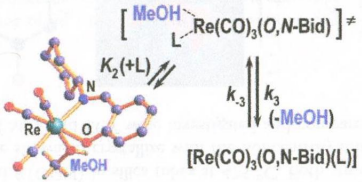

12489 S DOI: 10.1021/ic501603x

Chemical Bonding in a Linear Chromium Metal String Complex

Lai-Chin Wu, Maja K. Thomsen, Solveig R. Madsen, Mette Schmoekel, Mads R. V. Jørgensen, Ming-Chuan Cheng, Shie-Ming Peng, Yu-Sheng Chen, Jacob Overgaard,* and Bo B. Iversen*

A combined X-ray electron density and ab initio theoretical study has been carried out for the trichromium metal wire, $Cr_3(dpa)_4Cl_2\cdot(C_2H_5OC_2H_5)_x(CH_2Cl_2)_{1-x}$ (**1**, dpa = bis(2-pyridyl)amido)), and the chemical bonding is evaluated using both density and orbital based descriptors.

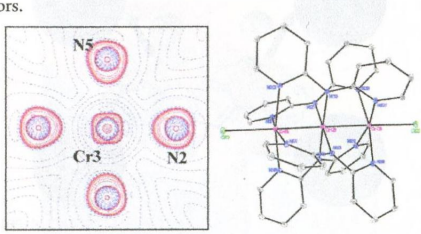

12499 S DOI: 10.1021/ic5020225

Lower Denticity Leading to Higher Stability: Structural and Solution Studies of Ln(III)–OBETA Complexes

Roberto Negri, Zsolt Baranyai, Lorenzo Tei, Giovanni B. Giovenzana,* Carlos Platas-Iglesias, Attila C. Bényei, Judit Bodnár, Adrienn Vágner, and Mauro Botta*

The heptadentate ligand OBETA (2,2′-oxybis(ethylamine)-*N*,*N*,*N*′,*N*′-tetraacetic acid) forms Ln^{3+} complexes with high thermodynamic stability and inertness, exceeding largely those of the complexes formed with the parent octadentate ligand EGTA. The presence of two water molecules coordinated to the metal ion in the Gd(OBETA) complex results in an important increase of its proton relaxivity. Thus, the OBETA scaffold represents an original platform for the development of improved contrast agents for application in MRI.

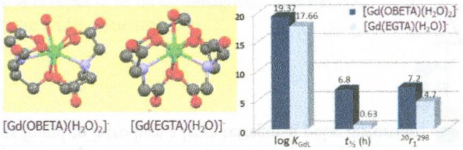

12512 S DOI: 10.1021/ic502026g

Ferrocenyl-Functionalized Sn/Se and Sn/Te Complexes: Synthesis, Reactivity, Optical, and Electronic Properties

Zhiliang You, Jakob Bergunde, Birgit Gerke, Rainer Pöttgen, and Stefanie Dehnen*

By treatment of $FcSnCl_3$ with K_2E (E = Se, Te), an adamantane-shaped, ferrocenyl-substituted tin selenide complex, $[FcSn_4Se_6]$ (**1**; Fc = ferrocenyl), and a ferrocenyl-substituted tin telluride five-membered ring, $[(Fc_2Sn)_3Te_2]$ (**2**), were synthesized. **1** can be further reacted with $Na_2S{\cdot}9H_2O$ and $[Cu(PPh_3)_3Cl]$ to form a ternary complex, $[(CuPPh_3)_6(S/Se)_6(SnFc)_2]$ (**3**). The title compounds were investigated by means of X-ray diffraction, UV–visible spectroscopy, cyclovoltammetry, and Mössbauer spectroscopy to gain insight into structural and electronic properties.

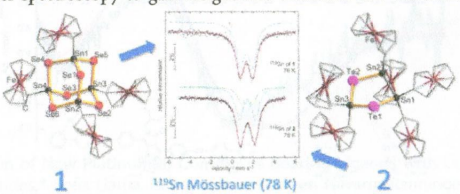

12519 S DOI: 10.1021/ic502063r

Interaction of Polycationic Ni(II)-Salophen Complexes with G-Quadruplex DNA

Laureline Lecarme, Enora Prado, Aurore De Rache, Marie-Laure Nicolau-Travers, Romaric Bonnet, Angeline van Der Heyden, Christian Philouze, Dennis Gomez, Jean-Louis Mergny, Hélène Jamet, Eric Defrancq, Olivier Jarjayes, and Fabrice Thomas*

Di- and tricationic nickel salophen complexes interact specifically with G-quadruplex DNA and inhibit telomerase. The two side chains connected at para positions of the phenol are inserted into opposite grooves of the G-quadruplex.

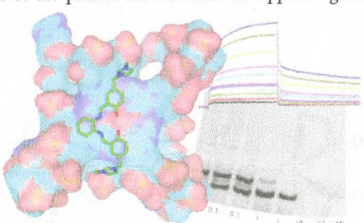

12532 S DOI: 10.1021/ic502088k

Solid-State Emissive B,S-Bridged *p*-Terphenyls: Synthesis, Properties, and Utility as Bifunctional Fluorescent Sensor for Hg^{2+} and F^- Ions

Dong-Mei Chen, Sheng Wang, Hong-Xiang Li, Xiao-Zhang Zhu, and Cui-Hua Zhao*

We disclosed a new class of ladder-type π-conjugated molecules, B,S-bridged *p*-terphenyls (**BS-TPs**), which are highly emissive in both solution and solid state and a display reversible reduction wave in cyclic voltammograms. In addition, this new class of ladder-type molecules are capable of simultaneous detection of F^- and Hg^{2+}, owing to the high Lewis acidity of the B center and the great mercury-philicity of the S center.

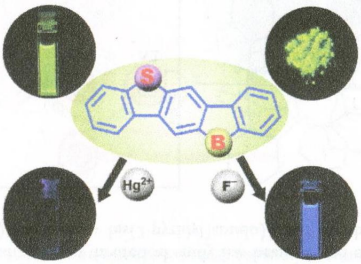

12540 S DOI: 10.1021/ic502035b

Synthesis and SHG Properties of Two New Cyanurates: $Sr_3(O_3C_3N_3)_2$ (SCY) and $Eu_3(O_3C_3N_3)_2$ (ECY)

Markus Kalmutzki, Markus Ströbele, Frank Wackenhut, Alfred J. Meixner, and H.-Jürgen Meyer*

The new cyanurates $Sr_3(O_3C_3N_3)_2$ (SCY) and $Eu_3(O_3C_3N_3)_2$ (ECY) were prepared via exothermic solid state metathesis reactions from MCl2 (M = Sr, Eu) and K(OCN) in silica tubes at 425 °C. Both structures were characterized by means of single crystal XRD. Their structures are shown to crystallize with the noncentrosymmetric space group *R3c* (No. 161). Nonlinear optical properties (NLO) of SCY and ECY were investigated and compared to those of CCY and β-BaB_2O_4 (β-BBO).

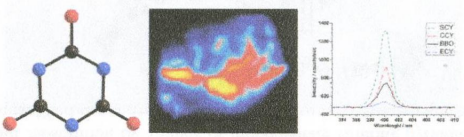

12546 S DOI: 10.1021/ic5021737

Synthetic-Method-Dependent Magnetic Relaxation in a Cobalt(II) Phosphonate Chain Compound

Zhong-Sheng Cai, Min Ren, Song-Song Bao, Norihisa Hoshino, Tomoyuki Akutagawa, and Li-Min Zheng*

Compound $Co(bamdpH_2)(H_2O)$ (**1**) [$bamdpH_4$ = ((benzylazanediyl)bis(methylene))diphosphonic acid, $C_6H_5CH_2N(CH_2PO_3H_2)_2$] displays independent canted antiferromagnetism but strong synthetic method dependence of the magnetic dynamics.

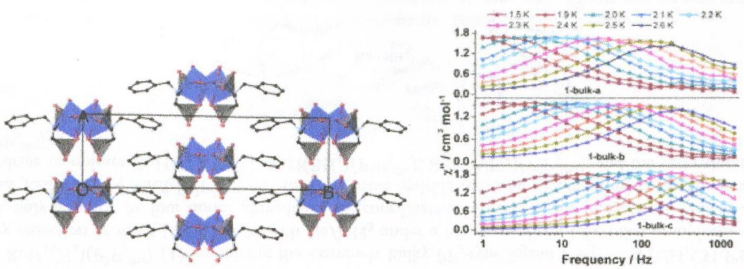

12553 S DOI: 10.1021/ic502181g

Reactivity of Bulky Formamidinatosamarium(II or III) Complexes with C=O and C=S Bonds

Glen B. Deacon,* Peter C. Junk,* Jun Wang, and Daniel Werner

Heteronuclear and homoleptic samarium(II) and samarium(III) formamidinato complexes react with benzophenone or CS_2 leading to some very unusual coupled species.

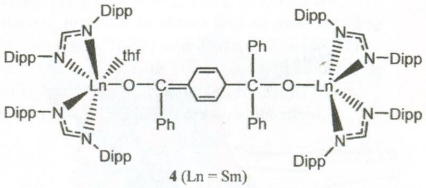

4 (Ln = Sm)
4Yb (Ln = Yb)

12564 S DOI: 10.1021/ic502169a

Triplet State Formation in Homo- and Heterometallic Diketopyrrolopyrrole Chromophores

Catherine E. McCusker, Delphine Hablot, Raymond Ziessel,* and Felix N. Castellano*

The synthesis, structural characterization, and excited-state dynamics of series of diketopyrrolopyrrole (DPP) bridged homodinuclear Ir(III) and heterodinuclear Ir(III)/Pt(II) complexes is presented. Steady-state and time-resolved photoluminescence along with transient absorption spectroscopy were used to probe the nature of the emissive and long-lived excited states. In all instances, ^{3}DPP*-localized excited states were observed in each molecule, regardless of the nature of the metal center or the number of coordinated metal centers.

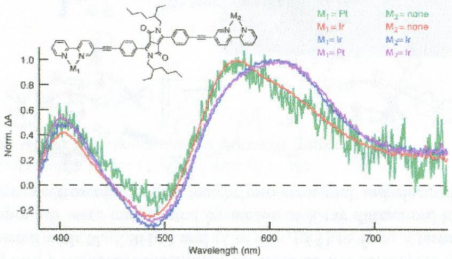

12572 S DOI: 10.1021/ic502183t

Introducing a Large Polar Tetragonal Distortion into Ba-Doped $BiFeO_3$ by Low-Temperature Fluorination

Oliver Clemens,* Robert Kruk, Eric A. Patterson, Christoph Loho, Christian Reitz, Adrian J. Wright, Kevin S. Knight, Horst Hahn, and Peter R. Slater

Ba-doping of $BiFeO_3$ followed by low-temperature fluorination to form compounds of composition $Bi_{1-x}Ba_xFeO_{3-x}F_x$ was found to introduce a large tetragonal polar distortion with $PbTiO_3$-type structure.

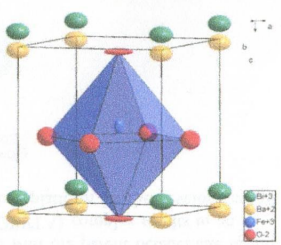

12584 S DOI: 10.1021/ic502202a

Lanthanum Lead Oxide Hydroxide Nitrates with a Nonlinear Optical Effect

Genxiang Wang, Min Luo, Chensheng Lin, Ning Ye,* Yuqiao Zhou, and Wendan Cheng

Two new lanthanum lead oxide hydroxide nitrates with NLO properties, $[LaPb_8O(OH)_{10}(H_2O)](NO_3)_7$ (**1**) and $[LaPb_8O(OH)_{10}(H_2O)](NO_3)_7{\cdot}2H_2O$ (**2**), have for the first time been obtained by the hydrothermal method, in which the novel $[LaPb_8O(OH)_{10}(H_2O)]^{7+}$ clusters present mirror symmetry. The cluster in compound **2** can change into that in compound **1** by the recombination of some bonds. The residue of compound **2** after efflorescence were confirmed to be compound **1**.

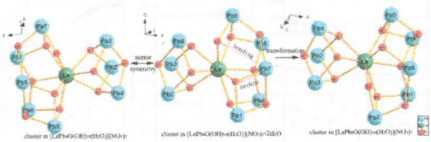

12590 S DOI: 10.1021/ic502223n

Water-Soluble Colorimetric and Ratiometric Fluorescent Probe for Selective Imaging of Palladium Species in Living Cells

Wei Liu, Jie Jiang, Chunyang Chen, Xiaoliang Tang, Jinmin Shi, Peng Zhang, Kaiming Zhang, Zhiqi Li, Wei Dou, Lizi Yang, and Weisheng Liu*

Based on palladium triggered cleavage reaction, a novel water-soluble colorimetric and ratiometric fluorescent probe was synthesized and applied for imaging palladium species (0, +2, +4) under physiological conditions in neutral PBS containing less than 1% organic cosolvent without any additional reagents. The probe exhibited a high selectivity, sensitivity for Pd^{2+}, with a noticeable color change and a low detection limit. The fluorescent ratiometric imaging of Pd^{2+} in living cells was also successfully carried out.

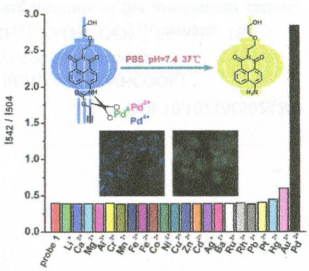

12595 S DOI: 10.1021/ic502239u

Effects of Terminal Dimethylation and Metal Coordination of Proline-2-formylpyridine Thiosemicarbazone Hybrids on Lipophilicity, Antiproliferative Activity, and hR2 RNR Inhibition

Felix Bacher, Orsolya Dömötör, Maria Kaltenbrunner, Miloš Mojović, Ana Popović-Bijelić, Astrid Gräslund, Andrew Ozarowski, Lana Filipovic, Sinisa Radulović, Éva A. Enyedy,* and Vladimir B. Arion*

Terminal dimethylation and copper(II) coordination of proline-2-formylpyridine thiosemicarbazone hybrids resulted in enhanced lipophilicity, antiproliferative activity in human cancer cell lines, and enhanced hR2 RNR inhibition.

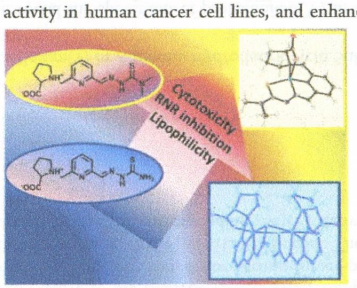

12610 S

DOI: 10.1021/ic502246p

Syntheses, Crystal Structures, Resistivity Studies, and Electronic Properties of Three New Barium Actinide Tellurides: $BaThTe_4$, $BaUTe_4$, and $BaUTe_6$

Jai Prakash, Sébastien Lebègue, Christos D. Malliakas, and James A. Ibers*

$BaThTe_4$, $BaUTe_4$, and $BaUTe_6$ have been synthesized and characterized. $BaThTe_4$ and $BaUTe_4$ are isostructural. The structure consists of $^2_\infty[AnTe_4^{2-}]$ layers (An = Th, U) separated by Ba^{2+} ions. The structure of $BaUTe_6$ features one-dimensional anionic $^1_\infty[U^{4+}(Te_2^{2-})_3^{2-}]$ chains separated by Ba^{2+} ions. From DFT calculations $BaThTe_4$ and $BaUTe_6$ are semiconductors consistent with resistivity measurements. $BaUTe_6$ is computed to be ferromagnetic, and $BaUTe_4$ is computed to be antiferromagnetic and a poor metal.

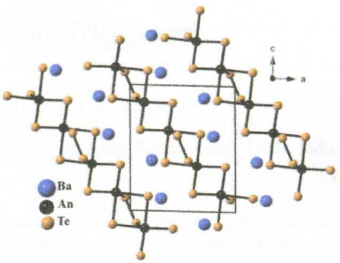

12617 S

DOI: 10.1021/ic502265g

Synthesis and Characterization of 12-Pyridinium Derivatives of the [*closo*-1-$CB_{11}H_{12}$]$^-$ Anion

Jacek Pecyna, Bryan Ringstrand, Sławomir Domagała, Piotr Kaszyński,* and Krzysztof Woźniak

12-(4-Pyridone-1-yl)-1-carbadodecaborates are convenient intermediates to polar liquid crystals and are obtained by diazotization of 12-amino-1-carbadodecaborates in 4-methoxypyridine solutions followed by removal of the methyl group with LiCl. The mechanism of their formation and the comparison of molecular and electronic structures of two isomeric 4-methoxypyridine derivatives of the [*closo*-1-$CB_{11}H_{12}$]$^-$ are discussed.

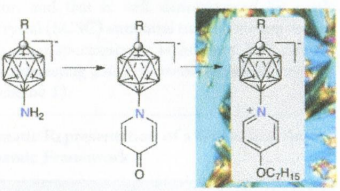

12627 S

DOI: 10.1021/ic502373n

Design and Biological Evaluation of New Platinum(II) Complexes Bearing Ligands with DNA-Targeting Ability

Jacqueline M. Herrera, Filipa Mendes,* Sofia Gama, Isabel Santos, Carmen Navarro Ranninger, Silvia Cabrera,* and Adoración G. Quiroga*

A novel series of *trans*-platinum(II) complexes bearing aliphatic amines and DNA-targeting ligands was synthesized to achieve more selective metallodrugs. The activity versus cancer cells of this series confirms the improvements of the six new complexes as they showed better cytotoxicity over the ligands and cisplatin.

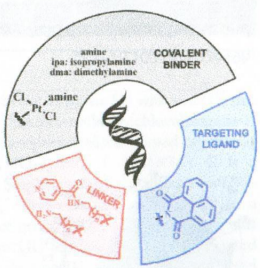

12635 S DOI: 10.1021/ic502375q

Formation of Difluorosulfane Complexes of the Third Row Transition Metals by Sulfur-to-Metal Fluorine Migration in Trifluorosulfane Metal Complexes: The Anomaly of Trifluorosulfane Iridium Tricarbonyl

Xiaozhen Gao, Nan Li,* and R. Bruce King*

The trifluorosulfane complexes $[M](SF_3)$ ($[M] = Ta(CO)_5$, $Re(CO)_4$, $CpW(CO)_2$, $CpOs(CO)$, and CpPt) are strongly thermodynamically disfavored relative to the isomeric $[M](SF_2)(F)$ complexes. The one anomaly is an $Ir(SF_3)(CO)_3$ isomer containing a one-electron donor pseudo-square-pyramidal SF_3 ligand having essentially the same energy as the lowest energy $Ir(SF_2)(F)(CO)_3$ isomer. The $[M](SF_2)(F)$ derivatives are viable toward SF_2 dissociation to give the corresponding $[M](F)$ derivatives.

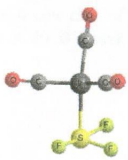

$Ir(SF_3)(CO)_3$

12643 DOI: 10.1021/ic502376m

EXAFS Study of the Speciation of Protactinium(V) in Aqueous Hydrofluoric Acid Solutions

Stéphanie M. De Sio and Richard E. Wilson*

X-ray absorption spectra of protactinium reveal the speciation of protactinium(V) in aqueous hydrofluoric acid (HF) solutions. The spectra show a changing coordination number from eight-coordinate to seven-coordinate and indicate a hydrated protactinium species at the lowest concentrations of aqueous HF, providing insight into the comparative chemistries of protactinium, its actinide brethren, and transition-metal homologues.

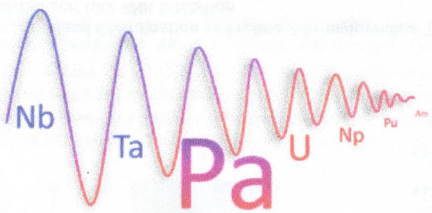

12650 S DOI: 10.1021/ic502426x

Raman and IR Studies of Pressure- and Temperature-Induced Phase Transitions in $[(CH_2)_3NH_2][Zn(HCOO)_3]$

Mirosław Mączka,* Tercio Almeida da Silva, Waldeci Paraguassu, Maciej Ptak, and Krzysztof Hermanowicz

We report temperature- and pressure-dependent Raman and IR studies of $[(CH_2)_3NH_2][Zn(HCOO)_3]$ formate. The temperature-induced phase transitions are associated with the freezing of ring-puckering motions of the azetidinium cation. This compound undergoes a phase transition near 0.4 GPa to the monoclinic phase. Two other phase transitions occur near 2.4 and 7.1 GPa. The first transition is associated with strong distortion of the framework and azetidinium cation, and the second one is associated mainly with distortion of the framework.

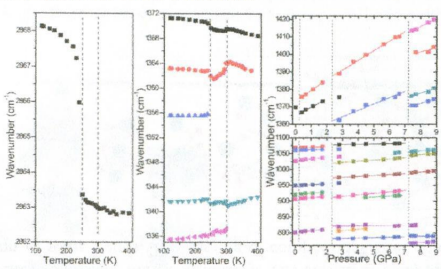

12658 Ⓢ

DOI: 10.1021/ic502443g

Field-Induced Multiple Relaxation Mechanism of $Co^{III}_2Dy^{III}$ Compound with the Dysprosium Ion in a Low-Symmetrical Environment

Shufang Xue, Liviu Ungur,* Yun-Nan Guo, Jinkui Tang,* and Liviu F. Chibotaru

A defective cubane-shaped heterometallic trinuclear $Co^{III}_2Dy^{III}$ compound, in which the Dy^{III} ion is in a low-symmetrical crystal field, displays field-induced multiple relaxation processes where are of molecular and a dipolar−dipolar coupling origin, as revealed by combined experimental and theoretical investigations.

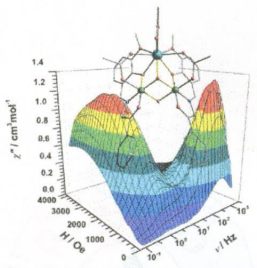

Additions and Corrections

12664

DOI: 10.1021/ic502449h

Correction to Photochemical Reactivity of the Iron(III) Complex of a Mixed-donor, α-Hydroxy Acid-Containing Chelate and Its Biological Relevance to Photoactive Marine Siderophores

Jennifer E. Grabo, Mark A. Chrisman, Lindsay M. Webb, and Michael J. Baldwin*

Ⓢ Supporting Information available via online article